molecule, the migrating group is bonded to a normal cycloheptatrienyl ring. The fact that there are now examples of two kinds of bonding in fluxional cycloheptatrienes should be considered in any structural decisions concerning new members of this interesting class of molecules.

Acknowledgment. The technical assistance of Y.-Y. Cheng is noted with appreciation.

Redetermination of the Structure of Porphine

Betty M. L. Chen and A. Tulinsky*

Contribution from the Departments of Chemistry and Biochemistry, Michigan State University, East Lansing, Michigan 48823.
Received September 18, 1971

Abstract: The structure of porphine has been redetermined with intensity measurements made in such a way as to optimize the reliability of the hydrogen atom structure, particularly that of the imino hydrogen atoms. The porphine molecule is composed of two like-opposite pairs of pyrroles rings, one pair of which carries imino hydrogen atoms. The different pairs of pyrroles show additional small but significant differences in bond distances and bond angles. The molecule is planar within about ±0.02 Å and possesses C_{2h} symmetry (approximate D_{2h} symmetry with the mirror planes bisecting the pyrrole rings). The different pyrroles are very similar to the two different pyrroles described in tetraphenylporphine. The structure of the free base macrocycle corresponds approximately with the hybrid of the two classical resonance forms of the porphine molecule. The new observations reported here were probably obscured in the original determination by the presence of a metalloporphine impurity.

As the parent compound of the porphyrin series, porphine occupies a unique position by virtue of its relative structural simplicity. Therefore, any comprehensive understanding of the structural interrelationships among the various members of the porphyrin series must rest intimately upon the fundamental understanding of the structural relationships within the simplest member itself. For such reasons, we have been concerned about the structure of the porphine molecule.

An X-ray crystallographic structure determination has been reported for the free base of porphine by Webb and Fleischer (hereafter referred to as W& F)[1] and the structure can be summarized briefly as (1) the macrocyclic ring (Figure 1) of four pyrroles alternately linked with bridging methine carbon atoms is essentially planar; (2) the average symmetry of the molecule corresponds closely to D_{4h} (4/*mmm*); and (3) the imino hydrogen atoms are apparently equally distributed among the four pyrrole rings and they are half-weight. The latter observations suggest the four pyrrole rings are equivalent and this has been atrributed to a rapid interconversion of N–H tautomers. Although this structure for porphine is certainly a plausible one, when it is compared with the free base of tetraphenylporphine (TPP)[2] and tetra-*n*-propylporphine (TPrP),[3] certain aspects of the porphine structure are perplexing: TPP and TPrP *have two localized imino hydrogen atoms on opposite pyrrole rings and these rings differ structurally from the other two pyrrole rings.* Such very different structural features for the porphine molecule are thus difficult to reconcile simply in terms of the substitution of phenyl or propyl groups for methine hydrogen atoms at the bridge positions.

Upon a more thorough and critical examination of the reported X-ray structure determination of porphine, it becomes clear that the work was unnecessarily complicated by the presence of an apparent metalloporphine impurity in the crystal which was used to collect the intensity data for the structure determination.[1] This fact was uncovered during the course of the structure analysis when a difference electron density map showed a residual peak of 2–3 electrons at the center of the molecule. The peak was ascribed to a metallo purity (5–10%) and it was included into least-squares refinement calculations as Cu^{2+} ion with partial occupancy. The atomic parameters of the impurity were then refined (multiplier, coordinates, anisotropic thermal parameters) and this resulted in considerable improvement in the agreement between the observed and calculated structure factors (decrease of about 0.09 in conventional R factor, $R = \Sigma||F|_o - |F|_c|/\Sigma|F|_o$). A difference electron density map based on a structure factor calculation *including the impurity* revealed 12 peaks averaging about 0.45 e Å^{-3} in peak height at the expected positions of the four methine and eight outer pyrrolic hydrogen atoms. The map also contained four slightly smaller peaks (averaging about 0.35 e Å^{-3} in height) near the center of the molecule and since these peaks had fairly reasonable positions with respect to the four pyrrole nitrogen atoms (0.8–0.9 Å), they were interpreted to be four half-hydrogen atoms corresponding to the imino hydrogen atoms of the pyrrole rings. Since the half-hydrogen atom result is a rather subtle one and in this case would depend upon how well the metallo impurity can be and was *removed from the observed data via calculation*, it is clear that under the circumstances, some of the foregoing procedures and results are questionable. Finally, the peak heights of the half-hydrogen atoms are too large compared to the full occupancy hydrogen atoms. This is all the more important since the final difference elec-

(1) L. E. Webb and E. B. Fleischer, *J. Chem. Phys.*, 43, 3100 (1965).
(2) S. J. Silvers and A. Tulinsky, *J. Amer. Chem. Soc.*, 89, 3331 (1967).
(3) P. W. Codding and A. Tulinsky, *ibid.*, 94, 4151 (1972).

tron density was said to contain random peaks of up to 0.2 e Å^{-3}, which is about the expected relative height of the half-hydrogen atoms.

Experimental Section

General. The porphine which was used in this work was prepared and purified (>99.9% porphine) by Dr. Alan D. Adler of the New England Institute. We are very grateful to Dr. Alder for providing us with such a fine sample of this material.

Single crystals of porphine were grown by slowly evaporating a solution of porphine in benzene which was kept dark by wrapping the container with aluminum foil. The crystals formed were dark-red pseudosquare platelets with the monoclinic unique b axis along one of the plate diagonals. Upon careful morphological examination of the crystals, a well-formed specimen with approximate dimensions of 0.28 × 0.20 × 0.05 mm was chosen for preliminary X-ray examination. The X-ray diffraction measurements showed the crystal to be of superior quality so it was used for most of the remainder of the work (a smaller crystal was used to correct for extinction effects). Crystals obtained in this way are: monoclinic, space group $P2_1/c$; four molecules per unit cell of dimensions a = 10.271 (3), b = 12.089 (3), c = 12.362 (4) Å; β = 102.17 (2)° (estimated standard deviations in parentheses).[4] These values are in good agreement with those reported by W & F.

Most of the X-ray work was carried out with a General Electric XRD-5 equipped with a quarter-circle single-crystal orienter and a scintillation counter assembly using Cu Kα radiation. Mosaic spreads of a number of representative reflections were measured to ensure that the crystal quality was sufficient for intensity data collection purposes and to aid in the choice of quadrant for data collection. All the spreads proved to be exceptionally symmetrical and less than 0.3° in width, from background to background, so the data collection quadrant was chosen on the basis of convenience (bounded by $\pm a^*$ and passing through c^*).

The intensities of the reflections were measured by the stationary crystal–stationary counter technique (SX). In order to avoid Kα_1 and Kα_2 splitting effects, the data collection was confined to reflections with scattering angles (2θ) less than 100°. This limit corresponds to about 1.0-Å resolution. The intensity of a reflection was measured with balanced Ni/Co filters and before each measurement, the angular settings were adjusted so that the intensity of the reflection was a maximum. The intensity was measured with a Ni filter at the adjusted angular settings for a 10-sec period followed by a similar measurement with a balanced Co filter. The intensity of the reflection was taken to be the difference between the Ni and the Co filter measurements. A total of 1725 reflections were measured in this manner, including 82 systematically absent ($h0l$) and 6 systematically absent ($0k0$) reflections. The average intensity for these 88 reflections was 5 counts/10 sec; consequently, only reflections greater than this count were taken to be observable. This resulted in 1206 (77%) independent observed reflections.

During the course of the intensity data collection, the intensities of three reflections were monitored as a function of X-ray exposure to the crystal (total of about 15 hr). The standard deviations from the average intensities for 32 measurements of the monitor reflections were 1.1, 1.2, and 1.8%. Thus, the crystal showed no loss in intensity due to exposure, the intensity of the X-ray source was constant for practical purposes, and the crystal remained well aligned throughout the data collection.

Absorption was corrected using a semiempirical method based upon the variation of relative transmission (T) with azimuthal angle (ϕ).[5] The $T(\phi)$ curves were obtained by measuring the variation of absorption of a reflection as the crystal was rotated about the normal to the corresponding reflecting planes. The b^* axis was at χ = 90° so ($0k0$) reflections were used to obtain the absorption correction of a general reflection in terms of ϕ, 2θ, and reciprocal lattice level (k index). However, since the (040) reflection was the only ($0k0$) reflection intense enough to be measured accurately, the absorption correction had to be confined to the use of the $T(\phi)$ curve of the (040) reflection. The maximum absorption ratio for this reflection (I_{max}/I_{min}) was about 1.1 and it occurred at the $\pm a^*$ axes.

Optimization of the Measurement of Hydrogen Contributions. Since the main interest of this redetermination of the structure of porphine was in the imino hydrogen atoms, it was desirable from the onset to carry out the necessary measurements in a way as to optimize the reliability of the final results. Methods for performing such an optimization have been discussed in some detail by Shoemaker[6] and we have applied some of these principles in an approximate way in this work. In addition to collecting a complete set of intensity data of the independent reflections by the SX technique, more elaborate counting techniques were applied to those reflections which were expected to have significant contributions from the hydrogen atoms of interest. Statistical counting errors would then be minimized for such reflections and the net result would be to give more precision in the parameters and structural features in question. The reflections which were expected to possess significant contributions from the imino hydrogen atoms and various possibilities thereof were ascertained through structure factor calculations based on the atomic parameters reported by W & F.

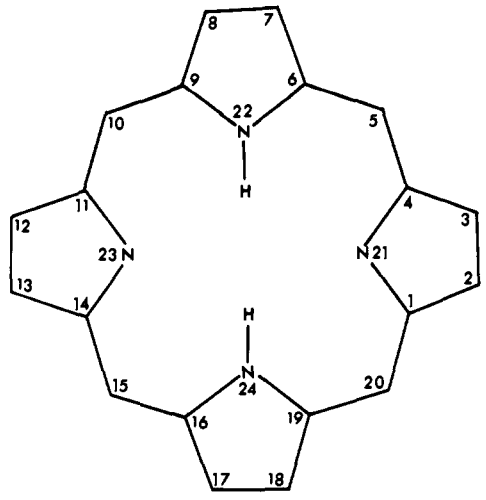

Figure 1. Numbering scheme for porphine (same as that of W & F).

The hydrogen atom structure factor calculations included the imino hydrogen atoms in three possible combinations and also the methine hydrogen atoms (numbering corresponds to that of W & F (Figure 1); the number of the hydrogen atom corresponds to the number of the atom to which it is bonded). The positional possibilities considered for the imino hydrogen atoms were (1) H_{21}–H_{23}, (2) H_{22}–H_{24}, and (3) a four half-hydrogen atom structure.[7] In addition, a calculation was performed with the methine hydrogen atom structure (H_5, H_{10}, H_{15}, H_{20}).[8] Since the mean value of the hydrogen scattering factor is less than 0.2 beyond $2\theta \geq 50°$, the structure factor calculations were confined below this limit. The distributions of the magnitudes of the different hydrogen atom contributions are shown in Figure 2, where the number of reflections with $|F_H| \geq 1.0$ in a given 2θ shell is shown as a function of scattering angle. From Figure 2, it can be seen that the largest number of significant hydrogen atom contributions is occurring in the 2θ = 30–40° scattering range; moreover, it can also be seen that the four half-hydrogen structure does not contribute very significantly to many reflections. Finally, it should be noted that the curves of Figure 2 do not fall off more abruptly because the number of possible reflections within a 2θ shell is rapidly increasing with Bragg angle.

The reflections which were assumed to possess a good hydrogen atom contribution and which were measured in a more extended way were decided upon according to the following scheme: $|F_H| > 2.0$ in at least one of the four hydrogen atom structures or $1.0 \leq |F_H| \leq 2.0$ for all four hydrogen atom structures. Of the 270 reflections in the range $2\theta < 50°$, about 10% were in the first category and about 20% in the second, giving a total of 80 reflections (hereafter referred to as the H reflections).

The intensities of the H reflections were remeasured using a step-scan procedure with the scan being symmetrically disposed about the peak of the reflection.[9,10] The scan was carried out in six incre-

(4) W & F chose the space group as $P2_1$ a; thus, the a and c axes of this work and that of W & F are interchanged.

(5) A. C. T. North, D. C. Phillips, and F. S. Mathews, *Acta Crystallogr., Sect. A*, 24, 351 (1968).

(6) D. P. Shoemaker, *ibid.*, 24, 136 (1968).

(7) $F(000)$ = 8.0 e.

(8) $F(000)$ = 16.0 e.

(9) H. W. Wyckoff, M. Doscher, D. Tsernoglou, T. Inagami, L. N.

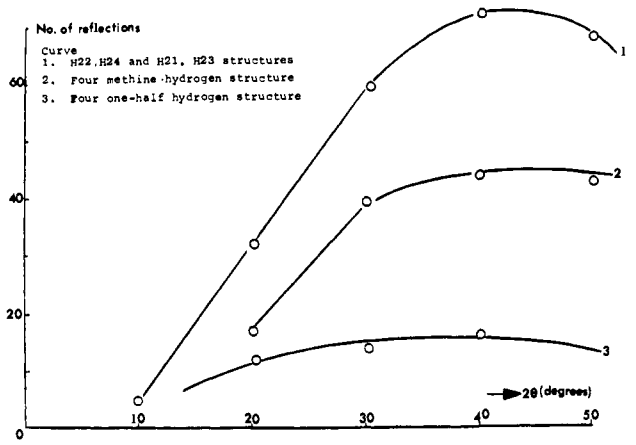

Figure 2. Distribution of various hydrogen atom contributions to the structure factor. Number of reflections were obtained as described in the text.

ments (0.04°) of ω, which is also the most sensitive angular dependence of a reflection. The intensity of a reflection was taken to be the sum of the four largest successive measurements using a Ni filter (count 6–drop 2). The background was then measured at the peak position with a Co filter.

Two methods of counting were used with the step-scan procedure depending upon the intensity of the reflection to be remeasured. The larger intensities, for which $I > 20$ counts/sec in the SX measurement, were remeasured using a constant accumulated count (CC) at each step; the smaller reflections, some of which might require inordinate counting times by the foregoing procedure, were remeasured using an increased constant counting time (CT). In order to keep the expected errors of the measurements somewhat comparable, several options were used for measurements and these were selected according to criteria given in Table I. The intensity

Table I. Counting Options of Step–Scan Measurement

Intensity (counts/sec of SX)	Counting method	Count at each step	Time at each step	Background at peak
<20	CT	I	10^2 sec	10^2 sec
$20 \leq I < 200$	CC	10^3	t	10^2 counts
$200 \leq I < 10^3$	CC	10^4	t	10^3 counts
$>10^3$	CC	10^5	t	10^4 counts

of the smaller reflections (CT) was based on a 400-sec counting time which was 40 times the counting time of the SX measurements. Simply on the basis of counting statistics, the remeasurement has an expected increase in precision of about $\sqrt{40}/40$ ($\sigma_{CT}(I) = 0.16\sigma_{SX}(I)$ or about a factor of 6). With the larger reflections, which were measured to a constant precision (CC), the accumulated count varied as given in Table I depending on the intensity of the reflection. In this way, the counting times were kept similar to each other and to those of the CT measurements. Moreover, the expected increase in precision for these reflections over the SX measurement was also approximately constant and about a factor of 3.

Since several intensity measuring techniques were used to obtain the intensity data, it became imperative to calibrate the various techniques to assure that systematic errors were not introduced due to scaling between the different sets of data. Calibrations between the SX–CT and SX–CC measurements were made by comparing the average ratio of the intensity measured by the different methods. The constants obtained were

$$\langle I_{SX}/I_{CT}\rangle_{n=24} = 0.99 \pm 0.06$$

$$\langle I_{SX}/I_{CC}\rangle_{n=54} = 1.00 \pm 0.04$$

where n is the number of reflections used in obtaining the average. Since both average ratios are unity within error, the reflections measured by the various methods were taken to be on the same scale.

An assessment of the agreement between the 80 H reflections measured by the different methods was made by evaluating a factor R_{SC-SX}

$$R_{SC-SX} = \sum|I_{SC} - I_{SX}|/\sum I$$

where SC and SX refer to intensities measured by the different methods and I is the average intensity of the two measurements. The largest discrepancy was about 9% but, in general, they were much smaller with $R_{SC-SX} = 0.026$ or about 0.013 with structure amplitudes. This shows the two sets of H reflection measurements to be essentially the same but since the intensities derived through the step-scan were in principle more reliable than those of the SX measurements, the latter were replaced with the former in the 1206 reflection set.

Structure Analysis

Initial Refinement. A trial structure based on the coordinates of W & F for the carbon and nitrogen atoms with an average individual isotropic temperature factor was used to compute an initial set of structure factors. The conventional R factor for this calculation was 0.142 and it decreased to 0.139 with one cycle of unit weight least-squares refinement of all the parameters. Electron and difference density maps were then computed using the signs of the larger calculated structure factors (1177 of 1206 reflections). The methine and outer pyrrolic hydrogen atoms (average peak height of about 0.5 e Å^{-3}) appeared in the difference density near expected positions; in addition, two peaks of 0.3 and 0.4 e Å^{-3} appeared within the center of the porphine ring which were also positionally correct to be imino hydrogen atoms bonded to the nitrogen atoms of opposite pyrrole rings. Since residual electron densities occurred in the vicinity of many of the atoms in this map, the least-squares refinement was continued with the use of individual anisotropic thermal parameters. Two cycles of refinement, the first including the inner 12 atoms and the second the outer 12 atoms, reduced R to 0.109. At this stage, examination of the observed and calculated structure factors indicated that most of the largest discrepancies were concentrated in some of the large low-order reflections. Since this is characteristic of primary and secondary extinction, some additional intensity measurements were made at this time with a smaller crystal before proceeding with the refinement.

Correction for Extinction. A smaller crystal with approximate dimensions of 0.12 × 0.15 × 0.025 mm (in a similar orientation to the larger crystal) was used to measure the intensities of reflections which might be affected by extinction. The volume ratio between the large crystal and the small crystal was 5.9. All the reflections bounded within the "hemisphere" $\pm h < 4$, $k \leq 4$, $l \leq 4$ were measured with the smaller crystal using a Picker four-circle automatic diffractometer controlled by a Digital Equipment Corp. (DEC) 4k PDP-8 computer (FACS-I System) coupled to a DEC 32k disk file. The intensities were measured by a "wandering" step-scan procedure and utilized balanced Ni/Co filters.[10] The intensities of the reflections from the smaller crystal were scaled to those of the larger crystal by comparing the intensities of some moderately large reflections which were obviously not affected by extinction. The scale constant obtained was

$$\langle|F_L|/|F_S|\rangle_{n=30} = 1.61 \pm 0.06$$

Johnson, K. D. Hardman, N. M. Allewell, D. M. Kelly, and F. M. Richards, *J. Mol. Biol.*, 27, 563 (1967).

(10) R. L. Vandlen and A. Tulinsky, *Acta Crystallogr., Sect. B*, 27, 437 (1971).

where $|F_L|$ and $|F_S|$ correspond to the large and small crystals, respectively, and n is the number of reflections used in the averaging. The agreement between the two crystals was assessed by evaluating the quantity R_{L-S}

$$R_{L-S} = \Sigma||F_L| - 1.61|F_S||/\Sigma|F|$$

where $|F|$ is the average structure amplitude of the two crystals; R_{L-S} was 0.033 for 188 reflections, excluding six large low-order reflections clearly affected by extinction. This value compares favorably with a similar agreement index obtained on comparison of ($\pm hk0$) equivalent reflections which were measured with the larger crystal; $R_L(hk0) = 0.020$ for 67 independent reflections. The agreement between these two sets is even more impressive considering that the structure amplitudes of the R_{L-S} comparison corresponded to two crystals with different dimensions, the intensities were measured by different methods (SX and CT step-scan), and the measurements were carried out with different X-ray diffractometers. Finally, it should be noted that the scale constant between the large and small crystal measurements does not correspond to the ratio of the volumes of the two crystals ($2.6 = (1.61)^2$ for the former and 5.9 for the latter). Since the quality of the diffraction pattern of the two crystals was apparently comparable, this difference is probably due to the more sensitive X-ray detection characteristics of the automatic diffractometer.

Six large low-order reflections of the larger crystal which showed pronounced extinction effects were replaced in the data set with the structure amplitudes obtained with the smaller crystal. These reflections are listed in Table II along with several pertinent structure amplitudes.

Table II. Reflections Corrected for Extinction

Reflection	$\|F\|_L$	$\|F\|_S$	$\|F_c\|^a$
022	137.5	160.6	167.0
$\bar{1}22$	95.5	111.1	111.1
013	89.7	99.8	100.6
023	116.3	129.7	133.5
$\bar{1}13$	107.0	122.3	123.5
$\bar{1}23$	155.2	172.8	181.8

[a] $|F_c|$ from final structure factor calculation including hydrogen atoms.

A structure factor calculation, including the six above reflections with new structure amplitudes but not including hydrogen atoms in the calculation, reduced R from 0.109 to 0.100. Another difference electron density was calculated from which the positions of all the hydrogen atoms were obtained. The hydrogen atoms were then included in a structure factor computation with individual isotropic thermal parameters which were approximated as 20% greater than the average temperature factor of the class of atom to which the hydrogen was bonded. This structure factor calculation gave $R = 0.086$ and one cycle of least-squares refinement of all the carbon and nitrogen atom coordinates reduced this value at 0.078. Another cycle of refinement varying the anisotropic thermal parameters of the *outer* 12 atoms decreased R to 0.072; varying similar parameters of the inner 12 atoms brought R to 0.068. The coordinates of the hydrogen atoms were then varied for one cycle and R improved slightly to 0.067. At this stage, a weighting scheme was introduced to complete the refinement.

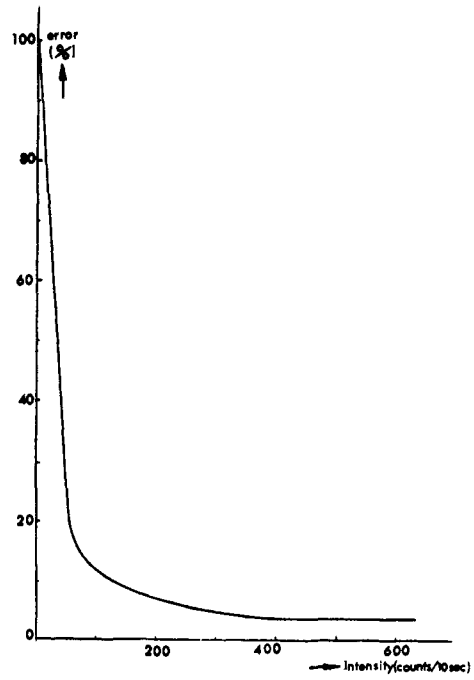

Figure 3. Per cent error curve used to obtain weights of smaller reflections ($400 \geq I > 5$) (curve derived as described in text).

Weighting Scheme. Three different weighting functions were used in the weighting scheme depending upon the intensity of the reflection. The factors taken into consideration were (1) counting statistics; (2) instrumental stability; and (3) assessments of the reliability of the measurements (various observed R factors).

(a) Unit weight reflections: $12{,}000 \geq I > 400$ (counts/10 sec).

$$\omega = 1/\sigma^2 = 1/(0.04|F|)^2$$

The data in this intensity range were generally very reliable so the error limit was assigned to be about twice the observed reproducibility of the monitored reflections.

(b) Large reflections: $I > 12{,}000$ (counts/10 sec).

$$\omega = (12{,}000/I) \times 1/(0.04|F|)^2$$

In this range, the error of the observation was assumed to increase with the magnitude of the observation; consequently, the reflections were downweighted in the weighting scheme. The reflections in this range were susceptible to extinction effects and to scaling errors, the latter arising because many of the reflections had to be measured at a reduced incident beam intensity in order to be within the linearity of the scintillation counter detector.

(c) Small reflections: $400 \geq I > 5$ (counts/10 sec).

The per cent error for reflections in this range was obtained graphically from the curve shown in Figure 3, which corresponds closely to constant error observations. The weight was taken to be

$$\omega = 1/(\%\ \text{error} \times |F|)^2$$

Table III. Final Atomic Parameters, Carbon and Nitrogen[a]

Atom	x	y	z	β_{11}	β_{22}	β_{33}	β_{12}	β_{13}	β_{23}	Peak height, e Å^{-3}
N(21)	0.1757 (3)	0.4670 (2)	0.1809 (2)	0.0121	0.0066	0.0063	0.0008	0.0023	−0.0001	7.6
C(1A)	0.3113 (4)	0.4476 (3)	0.1978 (3)	0.0112	0.0086	0.0071	−0.0006	0.0026	0.0014	6.2
C(2B)	0.3825 (4)	0.5359 (4)	0.2657 (3)	0.0148	0.0102	0.0072	0.0045	0.0015	−0.0002	5.9
C(3B)	0.2904 (5)	0.6068 (3)	0.2877 (3)	0.0177	0.0092	0.0071	−0.0041	0.0019	−0.0014	5.5
C(4A)	0.1613 (4)	0.5628 (4)	0.2353 (3)	0.0142	0.0076	0.0061	−0.0009	0.0017	0.0003	6.0
C(5M)	0.0418 (5)	0.6121 (3)	0.2388 (3)	0.0160	0.0067	0.0058	0.0007	0.0020	0.0006	6.0
N(22)	−0.1116 (3)	0.4801 (2)	0.1282 (2)	0.0113	0.0077	0.0065	0.0026	0.0025	0.0005	7.2
C(6A)	−0.0846 (4)	0.5743 (3)	0.1918 (3)	0.0151	0.0075	0.0057	0.0030	0.0029	0.0003	5.9
C(7B)	−0.2088 (5)	0.6244 (3)	0.1970 (3)	0.0186	0.0090	0.0077	0.0053	0.0038	0.0013	5.3
C(8B)	−0.3077 (4)	0.5598 (4)	0.1391 (3)	0.0135	0.0109	0.0076	0.0047	0.0041	0.0021	5.4
C(9A)	−0.2475 (4)	0.4672 (4)	0.0955 (3)	0.0091	0.0105	0.0066	0.0029	0.0021	0.0017	6.2
C(10M)	−0.3120 (5)	0.3826 (3)	0.0292 (3)	0.0102	0.0114	0.0070	−0.0004	0.0011	0.0013	5.8
N(23)	−0.1183 (3)	0.2774 (2)	0.0015 (2)	0.0103	0.0076	0.0069	0.0001	0.0017	0.0014	7.4
C(11A)	−0.2528 (4)	0.2954 (3)	−0.0144 (3)	0.0132	0.0083	0.0064	−0.0004	0.0022	0.0013	5.9
C(12B)	−0.3257 (4)	0.2091 (4)	−0.0855 (3)	0.0154	0.0097	0.0078	−0.0037	0.0010	0.0003	5.5
C(13B)	−0.2329 (5)	0.1405 (4)	−0.1098 (3)	0.0170	0.0092	0.0082	−0.0050	0.0013	0.0000	5.2
C(14A)	−0.1036 (4)	0.1824 (3)	−0.0580 (3)	0.0152	0.0070	0.0067	−0.0024	0.0015	0.0004	5.9
C(15M)	0.0173 (5)	0.1357 (3)	−0.0625 (3)	0.0151	0.0075	0.0074	−0.0013	0.0022	−0.0009	5.9
N(24)	0.1682 (3)	0.2672 (2)	0.0520 (2)	0.0104	0.0064	0.0070	0.0019	0.0024	0.0005	7.9
C(16A)	0.1424 (4)	0.1741 (3)	−0.0141 (3)	0.0151	0.0055	0.0068	0.0021	0.0034	0.0000	6.0
C(17B)	0.2661 (5)	0.1231 (4)	−0.0197 (3)	0.0185	0.0081	0.0089	0.0052	0.0041	0.0011	5.7
C(18B)	0.3661 (5)	0.1863 (4)	0.0410 (4)	0.0159	0.0077	0.0085	0.0049	0.0043	0.0018	5.6
C(19A)	0.3047 (4)	0.2768 (3)	0.0862 (3)	0.0112	0.0074	0.0068	0.0021	0.0029	0.0024	6.1
C(20M)	0.3700 (4)	0.3597 (3)	0.1560 (3)	0.0099	0.0091	0.0074	0.0001	0.0021	0.0015	5.9
$\sigma \times 10^5$	27–51	20–38	22–35	51–75	35–55	34–52	36–55	35–53	27–40	

[a] Anisotropic temperature factor = $\exp[-(\beta_{11}h^2 + \beta_{22}k^2 + \beta_{33}l^2 + 2\beta_{12}hk + 2\beta_{13}hl + 2\beta_{23}kl)]$. Standard errors of coordinates in parentheses.

The per cent error curve was constructed by considering observed behavior at selected points in the intensity range. The boundary conditions of the curve were chosen such that the relative errors of $I = 400$ and $I = 5$ corresponded to 4 and 100%, respectively. Thus, the errors in this range merged asymptotically with the error of unit weight reflections. Three other points were fixed on the per cent error curve according to the following considerations: (1) at $I = 68$, per cent error = 15%; this was the maximum counting error observed for the (306) reflection (measured a number of times); (2) at $I = 234$, per cent error = 8%; this was the counting error observed for the (110) reflection, which was the largest error shown among the reflections in this counting range; and (3) at $I = 300$, per cent error = 5%; this was the counting error of the ($\bar{4}25$) reflection considered to be representative of reflections in this counting range.

The weighting scheme was then included in the least-squares refinement and after two cycles of varying the atomic coordinates followed by the anisotropic thermal parameters of the carbon and nitrogen atoms, the R factor decreased from 0.067 to 0.059 and the weighted R factor was 0.041. Since a cycle of refinement of hydrogen atom coordinates had negligible shifts and no other apparent effects, the refinement of the structure was terminated at this point.

Two additional structure factor calculations were carried out at this time to assess the effect of the hydrogen atom contributions on the structure. The first calculation did not include the imino hydrogens (H_{22}, H_{24}) and R increased significantly to 0.066; the second calculation did not include any of the hydrogen atoms (total of 14) and R increased very significantly to 0.093.

Results[11]

The final atomic parameters of the carbon and nitrogen atoms of porphine are listed in Table III, while those of the hydrogen atoms are given in Table IV.

Table IV. Final Hydrogen Atom Parameters

Atom	x	y	z	Peak height, e Å^{-3}
H(22)	−0.0483	0.4375	0.1192	0.5
H(24)	0.1067	0.3133	0.0600	0.5
H(2B)	0.5149	0.0358	0.2108	0.5
H(3B)	0.7055	0.1751	0.1632	0.5
H(5M)	0.9614	0.1763	0.2187	0.5
H(7B)	0.2149	0.1902	0.2675	0.5
H(8B)	0.4133	0.0634	0.3705	0.6
H(10M)	0.5760	0.3860	0.0153	0.5
H(12B)	0.5637	0.2832	0.3916	0.4
H(13B)	0.7435	0.4238	0.3298	0.5
H(15M)	0.0151	0.4327	0.3803	0.5
H(17B)	0.2867	0.4435	0.4337	0.5
H(18B)	0.4784	0.1723	0.0603	0.5
H(20M)	0.4848	0.3465	0.1696	0.6

The fluctuation of the standard deviations obtained from the least-squares procedure for the atomic parameters of the carbon and nitrogen atoms is given in the last row of Table III. The standard deviations of the hydrogen atom coordinates are about 10 times greater than the atoms to which they are bonded.

A plane was fitted to the 24 carbon and nitrogen atoms of the porphine molecule by the method of least squares. The deviations of the atoms from this plane

(11) Copies of the observed and calculated structure amplitudes are available from one of the authors (A. T.) upon request.

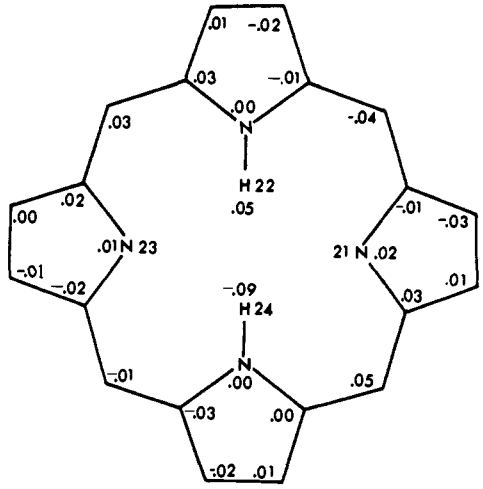

Figure 4. Deviations from nuclear least-squares plane (in ångströms).

(NLS) are shown in Figure 4 (standard deviation of 0.02 Å); for comparison, the deviations of the atoms from the best least-squares plane of each individual pyrrole ring are listed in Table V. Thus, the individual

Table V. Atomic Deviations from Least-Squares Planes of Individual Pyrrole Rings

Pyrrole N21		Pyrrole N22	
N21	−0.002	N22	−0.008
C1	−0.002	C6	0.007
C2	0.004	C7	−0.003
C3	−0.005	C8	−0.002
C4	0.004	C9	0.006
σ =	0.003	σ =	0.006
Pyrrole N23		**Pyrrole N24**	
N23	0.004	N24	0.004
11	0.001	16	−0.006
12	−0.005	17	0.005
13	0.008	18	−0.002
14	−0.007	19	−0.001
σ =	0.005	σ =	0.004

pyrrole rings are planar and the porphine molecule itself is planar within ±0.02 Å. The latter is close to the error of the determination of the least-squares plane.

The interatomic bond distances and bond angles of porphine are shown in Figures 5 and 6, respectively. The standard deviations of the bond lengths and bond angles involving carbon and nitrogen atoms are estimated to be 0.004–0.007 Å, and 0.3–0.5°, respectively, and are based on the standard deviations of the atomic coordinates of the final cycle of least-squares refinement.

The composite final difference electron density of the hydrogen atoms of porphine viewed along the b^* direction is shown in Figure 7. The structure factor calculation for this electron density map was based on the final carbon and nitrogen atom structure and did not include the hydrogen atoms (R = 0.093). The standard deviation of this difference electron density is about 0.1 e Å^{-3}.

Discussion

From Figure 7, it can be seen that all 14 hydrogen atoms of the porphine molecule appear clearly in a similar way and to the same extent in the final difference electron density map, *including two localized imino hydrogen atoms* which indicate that the pyrroles differ from one another in like pairs. From Figure 5, it can be seen that the average C–H distance is 1.06 ± 0.08 Å, excluding the imino hydrogens which show a significantly smaller distance of 0.86 Å. A similar shortening in the imino hydrogen distance was observed in TPP (N–H = 0.93 Å) and must be due in part to the intrinsic difference between a C–H and N–H bond length. In addition, the imino hydrogen atoms of porphine are displaced slightly above and below the NLS plane of the molecule (H_{22} = +0.05, H_{24} = −0.9 Å; Figure 4) and the ∠CNH angles are distorted from a symmetrical trigonal array (Figure 6). The net effect of all of these factors on the imino hydrogens is to increase the distance between these two hydrogen atoms. This distance is 2.41 Å and compares well with the 2.36-Å separation observed in TPP.

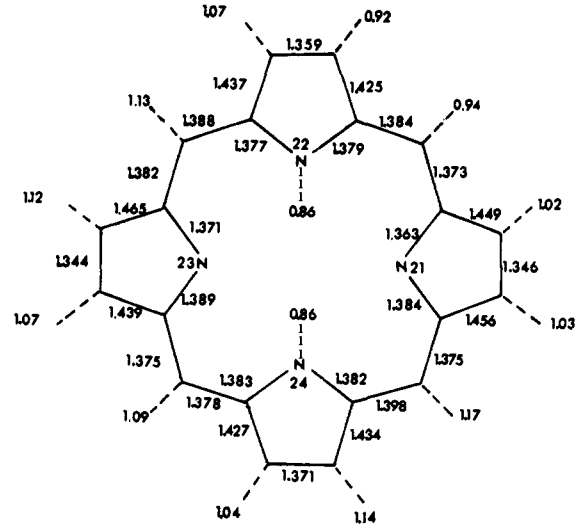

Figure 5. Bond distances (in ångströms) for porphine. Bonds to hydrogen atoms broken.

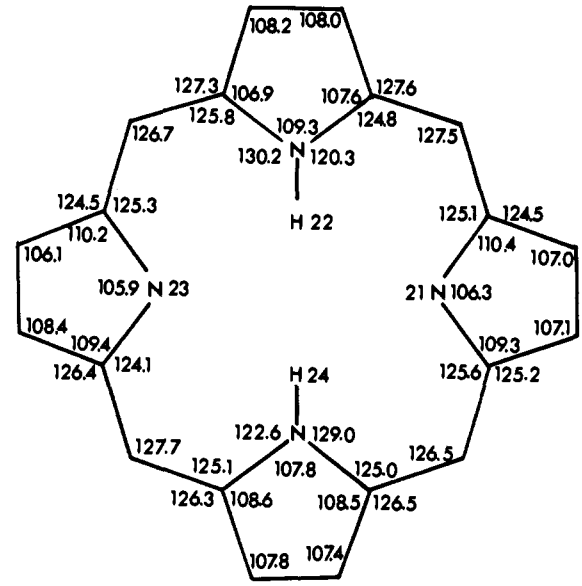

Figure 6. Bond angles (in degrees) for porphine.

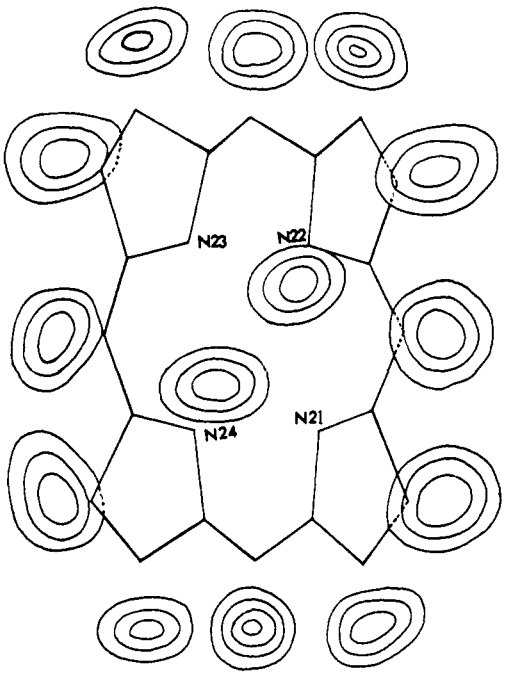

Figure 7. Composite difference electron density of the hydrogen atoms: viewed perpendicular to *ac* plane; contours at 0.15 e Å^{-3} beginning at 0.15 e Å^{-3}.

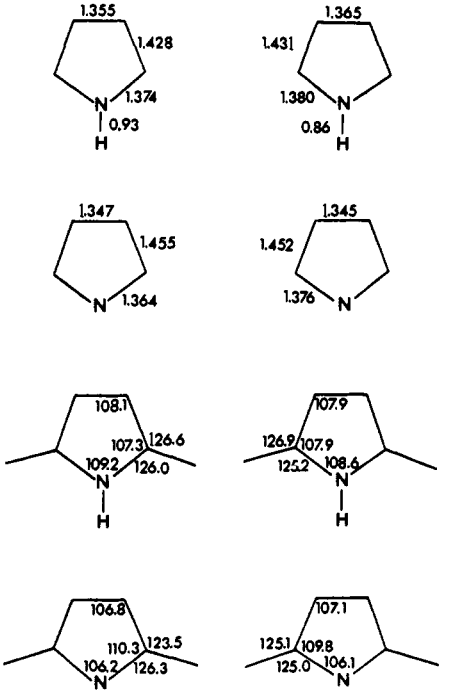

Figure 8. Comparison of average bond distances and angles of independent pyrroles of porphine and TPP: TPP on left; porphine on right.

The deviations of the atoms from the NLS plane are relatively small and, to a first approximation, the molecule can be considered planar (±0.02 Å). This strongly suggests that the lack of planarity observed in TPP is probably due to the close intermolecular contact of a phenyl group carbon atom to the nitrogen atom of the reduced pyrrole ring rather than due to a repulsion effect arising from the close contact of the imino hydrogen atoms.[2] The particular contact in question is 3.40 Å which is fairly small for a van der Waals distance and is the smallest intermolecular approach observed in TPP. Finally, a closer examination of the distribution of the deviations from planarity of porphine (excluding the imino hydrogens of Figure 4) reveals that they approximate C_{2v} symmetry with the mirror planes passing through the methine carbon atoms. However, the full significance of this symmetry is difficult to assess since the deviations border on the limits of the errors of the determination.

From Figures 5 and 6, it can be seen that the pyrrole rings of porphine differ in like pairs that are opposite one another and since the molcule is approximately planar, the molecule possesses good C_{2h} symmetry with respect to its geometry (bond distances and bond angles) and approximate D_{2h} symmetry with the mirror planes bisecting the pyrrole rings. The geometries of the independent pyrrole rings of porphine are strikingly similar to those of TPP[2] and TPrP[3] and they correspond approximately to a structure expected of a hybrid of the two predominant resonance forms of the macrocyclic ring system originally suggested for the structure of TPP. A comparison of the average bond distances and bond angles of the independent pyrroles of porphine and TPP is shown in Figure 8 from which it can be seen that they are very similar. The only significant difference occurs in the average bond angles involving the C_α and methine carbon atom of the azapyrrole ring. This difference might be the result of packing effects arising from the phenyl rings of TPP but which have no counterpart with porphine.

Concluding Remarks

A comparison has been made of the observed structure amplitudes employed in this work with those used by W & F. The comparison was carried out by evaluating an R_D factor

$$R_D = \sum^{N} ||F_o| - |F|_{WF}| / \Sigma |F_o|$$

where $|F_o|$ and $|F|_{WF}$ are the observed structure amplitudes of the present and the W & F work, respectively, and the summation extends over the 1206 observations of the present work, with $\Sigma^N|F_o| \simeq \Sigma^N|F|_{WF}$. The value of the R_D factor is 0.13 and indicates a substantial difference between the two sets of data. The difference is probably due to the metallo impurity contribution in the data of W & F. It is interesting to note that the inclusion of the metal impurity into structure factor calculations by W & F resulted in a decrease of the conventional R factor of about 0.09.[1] On this basis, with the metal impurity contribution removed from the data, the W & F data might be comparable to that of the present work.

On the other hand, another viewpoint can be assumed which would suggest that the W & F results are, at least, approximately correct.[12] It is known that two complete series of solid solutions exist between TPP and its silver(II) derivative (AgTPP).[13] One series possesses a triclinic structure, the other a tetragonal one,

(12) We would like to thank the referee for bringing this to our attention.

(13) Dr. Gabrielle Donnay, private communication to the referee and one of us (A. T.); also, M. L. Schneider and G. Donnay, Abstracts, Summer Meeting of the American Crystallographic Association, Ames, Iowa, Aug 1971, No. K14.

with crystals of both emerging simultaneously from the same solution. The tetragonal form would imply rapid interconversion of N–H tautomers or stacking disorder in the crystal.[14] Thus, it seems as if the presence of an impurity such as Ag(II) can induce one or the other of these, which ultimately leads to effectively fourfold symmetry. It is possible, therefore, that the Cu(II) impurity in the W & F crystals of porphine might also be effective in this connection in a monoclinic case.

(14) M. J. Hamor, T. A. Hamor, and J. L. Hoard, *J. Amer. Chem. Soc.*, **86**, 1938 (1964).

Acknowledgment. We would like to take the opportunity here to gratefully acknowledge the support of this work by the National Science Foundation, Molecular Biology Section (Grants GB-5686, GB-7399, and GB-15402). In addition, we would like to thank Mr. Richard L. Vandlen for the many ways he has contributed to all aspects of this work.

Structure of Tetra-*n*-propylporphine. An Average Structure for the Free Base Macrocycle from Three Independent Determinations

Penelope W. Codding[1] and A. Tulinsky*

Contribution from the Departments of Chemistry and Biochemistry, Michigan State University, East Lansing, Michigan 48823. *Received September 18, 1971*

Abstract: The crystal and molecular structure of $\alpha,\beta,\gamma,\delta$-tetra-*n*-propylporphine has been solved using X-ray crystallographic techniques. The structure was solved using Sayre's equation. The molecule is centrosymmetric with two independent pyrrole rings. A common structure for the free base macrocycle was obtained by averaging from the tetraphenylporphine, porphine, and tetrapropylporphine determinations. The free base structure consists of opposite pyrrole rings possessing imino hydrogen atoms and the pyrrole rings differing in like pairs. Small differences which are localized at the bridge carbon atoms were found for the substituted compounds. In addition, the aliphatic substituent seems to decrease some of the differences between the two pyrrole rings. The individual pyrrole rings are planar to ±0.007 Å and the nucleus of the tetrapropylporphine ring is essentially planar (±0.04 Å). Some small deviations from planarity are probably due to packing effects with the closest intermolecular distance being 3.36 Å. The propyl groups are in an extended configuration efficiently filling the space between molecules in the crystal.

From the X-ray crystallographic structure determinations of two synthetic free base porphyrins, triclinic tetraphenylporphine (TPP)[2] and porphine,[3] there are indications that a common structure exists for the macrocyclic ring system of four alternate pyrrole rings joined by methine carbon atom brdiges. This structure consists of opposite pyrrole rings possessing imino hydrogen atoms with small structural differences between these rings and the other two pyrrole rings (in bond distances and bond angles). At the time when this work was begun, the redetermination of the structure of porphine was not yet completed so that there were two main objectives in the structure determination of $\alpha,\beta,\gamma,\delta$-tetra-*n*-propylporphine (TPrP): (1) to obtain an accurate structure of the free base macrocycle and (2) to try to determine the effect of an aliphatic substitution on the free base structure by comparing the structure of TPrP with that of TPP and porphine. Extensive studies of the visible spectra of porphyrins have shown that a correlation exists between the positions and relative intensities of the visible absorption bands and the nature of the side chains at various substitution positions on the macrocycle. These studies suggest that different changes in the π-electron density of the macrocycle are caused by different substituents.[4] Since the electronic effects of an aromatic (TPP) and an aliphatic substitution (TPrP) are fairly different (Figure 1), under favorable circumstances, a comparison of these two structures with that of porphine could lead to some insight concerning changes occurring in the π-electron density accompanying substitution of the porphine ring. The extent to which this has been accomplished will be clear from the results to be reported here.

(1) NDEA Title IV Fellow, 1969–1971.
(2) S. J. Silvers and A. Tulinsky, *J. Amer. Chem. Soc.*, **89**, 3331 (1967).
(3) B. M. L. Chen and A. Tulinsky, *ibid.*, **94**, 4144 (1972).

Experimental Section

Single crystals of TPrP in the form of purple hexagonal prisms were grown by slowly evaporating a saturated benzene solution of TPrP.[5] A suitable crystal with approximate dimensions of 0.15 mm in all directions was selected for X-ray examination. Preliminary X-ray diffraction measurements showed the crystal to be monoclinic with unit cell dimensions of $a = 5.078\,(5)$, $b = 11.59\,(2)$, $c = 22.39\,(3)$ Å; $\beta = 99.50\,(5)°$. Systematic absences fixed the space group to be $P2_1/c$. The calculated density of the crystal on the basis of two molecules per unit cell is 1.223 g cm^{-3} and the observed density measured by flotation in aqueous silver nitrate solution is 1.22 (1) g cm^{-3}.

All the X-ray measurements and the intensity data collection were made with Cu Kα radiation using a Picker four-circle automatic X-ray diffractometer controlled by a Ditigal Equipment Corp. (DEC) 4K PDP-8 computer (FACS-I System) coupled to a DEC 32K

(4) For a review of spectral studies of porphyrins, see J. E. Falk, "Porphyrins and Metalloporphyrins," Elsevier, Amsterdam, 1964, Chapter 6.
(5) We would like to thank Dr. Alan D. Adler of the New England Institute for kindly supplying us with a sample of TPrP.